Nanoscale

Mucus barrier-triggered disassembly of siRNA nanocarriers

Journal:	*Nanoscale*
Manuscript ID:	NR-ART-03-2014-001584.R1
Article Type:	Paper
Date Submitted by the Author:	06-Aug-2014
Complete List of Authors:	Thomsen, Troels; Interdisciplinary Nanoscience Center, Li, Leon; MIT, Howard, Ken; Aarhus University, Interdisciplinary Nanoscience Center (iNANO)

Cite this: DOI: 10.1039/c0xx00000x

www.rsc.org/xxxxxx

ARTICLE TYPE

Mucus barrier-triggered disassembly of siRNA nanocarriers

Troels B. Thomsen[a,b], Leon Li[c,d,e], Kenneth A. Howard*[a,b]

Received (in XXX, XXX) Xth XXXXXXXXX 20XX, Accepted Xth XXXXXXXXX 20XX
DOI: 10.1039/b000000x

The mucus overlying mucosal epithelial surfaces presents not only a biological barrier to the penetration of potential pathogens, but also therapeutic modalities including RNAi-based nanocarriers. Movement of nanomedicines across the mucus barriers of the gastrointestinal mucosa is modulated by interactions of the nanomedicine carriers with mucin glycoproteins inside the mucus barriers potentiated by the large surface area of the nanocarrier We have developed a fluorescence activation-based reporter system showing that the interaction between polyanionic mucins and the cationic chitosan/small interfering RNA (siRNA) nanocarriers results in the disassembly and consequent triggered release of fluorescent siRNA. The quantity of release was found to be dependent on the molar ratio between chitosan amino groups and siRNA phosphate groups (NP ratio) of the polyplexes with a maximal estimated 48.6% release of siRNA over 30 min at NP 60. Furthermore, a microfluidic in vitro model of the gastrointestinal mucus barrier was used to visualize the dynamic interaction between chitosan/siRNA nanocarriers and native purified porcine stomach mucins. We observed strong interactions and aggregations at the mucin/liquid interface, followed by an NP ratio dependent release and consequent diffusion of siRNA across the mucin barrier. This work describes a new model of interaction at the nanocarrier/mucin interface and has important implications for the design and development of nucleic acid-based nanocarrier therapeutics for mucosal disease treatments and insights into nanoscale pathogenic processes.

1. Introduction

The posttranscriptional inhibition of protein expression by the process of RNA interference (RNAi) offers an attractive therapeutic strategy for many diseases including cancer, neurological disorders and mucosal diseases.[1, 2] Gene specificity through complementary base pairing between small interfering RNA (siRNA) and messenger RNA (mRNA) combined with the ability to engage and harness the cellular RNAi pathway using a wide repertoire of RNAi-based therapeutics drives RNAi drug development. The delivery of RNAi-based therapeutics across mucosal surfaces that line the gastrointestinal, respiratory and genitourinary tract is an attractive route of administration as it allows direct access to the site of mucosal diseases and can result in systemic translocation.[3, 4] Ease of administration and increased patient compliance and cost-effectiveness promotes the oral route, particularly for treatment of pathological conditions local to the gastrointestinal tract (GI tract) mucosa such as Inflammatory Bowel Disease.[5] However, successful clinical translation of oral RNAi-based therapeutics has been limited by the susceptibility of siRNA to nuclease degradation in the harsh conditions of the gastrointestinal tract and the poor cellular uptake of polyanionic siRNA. Polymer based polyelectrolyte nanocarriers (termed polyplexes) are submicron nanoparticles formed by electrostatic self-assembly between cationic polymers and anionic nucleic acid cargo which have been developed for protection and delivery of small interfering RNA (siRNA).[6-8] Chitosan is a natural cationic material shown to facilitate the opening of epithelial tight-junctions[9] and exhibit mucoadhesive properties[10, 11] that promotes inclusion into the nanocarrier design for siRNA delivery targeted at the gastrointestinal mucosa. We have previously shown protection and intestinal luminal deposition of siRNA after oral administration using chitosan/siRNA nanocarriers.[12]

The mucus overlying mucosal epithelial surfaces presents an innate and significant biological barrier to the penetration of therapeutic modalities including RNAi-based nanocarriers. The main structural components of this highly hydrated and viscous gel are glycoproteins termed mucins[13] that form a heterogeneous network of polymeric fibres and pores through which particles need to diffuse. Hydrophilic glycosylated amino acid sequences and hydrophobic cysteine-rich domains in the mucin fibers are available for electrostatic, hydrogen and hydrophobic interactions with particles.[14] The particle size and chemical surface properties of the nanocarriers, therefore, determine diffusion through the mucus layer.[15] Electrostatic interactions of the cationic polymer component of polyplex nanocarriers with mucins play an important role for the mucoadhesive properties[16] thought to increase at higher NP ratio (ratio of cationic amino groups to RNA-bearing anionic phosphates). While previous studies have characterized the intracellular release kinetics of polyplexes[17] together with the parameters governing intracellular release[18] and gene silencing,[7] polyplex stability and integrity after interaction with the mucus barrier has not been investigated.

In this study, we investigate the integrity of chitosan/siRNA polyplex nanocarriers in gastrointestinal mucins using a

fluorescence activation-based reporter stability assay and a microfluidic mucus barrier model. The reversible quenching of fluorescence at elevated dye concentrations or labeling densities is a recognized phenomena which has been used to study liposome-cell[19] and vesicle-vesicle fusion,[20] protease activity,[21] protein folding,[22] and pH sensitive nanoparticles.[23, 24] Self-quenching between identical fluorophores occurs when fluorophores are in a condensed state and involves a combination of trap-site formation and resonance energy transfer between the fluorophores due to a small stokes shift.[23, 25] We have developed a fluorescence activation reporter system for evaluating nanocarrier integrity based on fluorescence self-quenching on particle assembly as a result of the close proximity of the dye molecules on the different siRNA, and subsequent activation of the fluorescent signal following disassembly. Furthermore we have developed a microfluidic mucus barrier model, previously employed to measure the barrier properties of mucins towards gastric juices[26] and peptides[27], for a novel application to study the real-time dynamic interaction between moving nanocarriers and the luminal site of the mucus barrier. Overall, our results demonstrate, for the first time, the decomplexation and the consequent release and diffusion of the constituent siRNA after interaction of the polyplex nanocarriers with gastrointestinal mucins. We further show that the decomplexation and transport kinetics is influenced by mucin concentration, mucin-nanocarrier interaction time, and nanocarrier formulations that provide design guidelines for RNAi-based nanocarrier therapy targeted at mucosal sites. In addition findings from this work have important implications into interpreting transport properties of nanoscale pathogens exhibiting similar surface properties.

2. Experimental section

Materials

siRNA duplexes labeled at the 5' end of the sense strand with 5-carboxyfluorescein (5-FAM) dye were purchased from Genepharma (Shanghai, CH). The sequences were: sense 5'-(5-FAM)-GGUCAUCCAUGACAACUUUTT-3', antisense 5'-AAAGUUGUCAUGGAUGACCTT-3'. Heparin was purchased from Sigma Aldrich. Porcine gastric mucins were either purified from pig stomach scrapings according to Celli et al.,[28] except that the caesium chloride density gradient ultracentrifugation step was omitted, or purchased from Sigma Aldrich (Type III). Chitosan (M_w = 58 kDa, degree of deacetylation = 81.3%) was obtained from Kitozyme (Belgium).

Particle formation and characterization

Particles were prepared as previously described.[29] Briefly, chitosan was dissolved in sodium acetate buffer (pH = 5.5, 300 mM) to give a concentration of 1 mg/mL and filtered prior to use. Nanocarriers were formed by adding 5-FAM labeled siRNA (siRNA-FAM) (100 μM) in nuclease-free water to 500 μL chitosan solution (0.72 μg/mL) whilst stirring for 1h. The amount of chitosan was varied while keeping the amount of siRNA constant to produce nanoparticles of NP ratio ranging from 0.5 to 60. The hydrodynamic radius and zeta potential of the nanoparticles were determined using Dynamic Light Scattering (DLS) (Zetasizer Nano ZS, Malvern, UK) performed in sodium acetate buffer at 25 ^{o}C with measurements in triplicate with sampling time and analysis set to automatic.

Fluorescence activation assays

Porcine gastric mucins (Type III, Sigma Aldrich) were hydrated o/n in deionised water and dialysed against deionised water for 72 h at 4 ^{o}C before being lyophilized. The lyophilized mucins were reconstituted in a simulated physiological intestinal fluid prepared according to the International Pharmacopoeia; SIF, 50.3 mmoles of potassium dihydrogen phosphate and 38 mmoles of sodium hydroxide were dissolved in Milli-Q water, adjusted to a final pH of 7.5 with sodium hydroxide (0.2 mol/L) and diluted to produce 1litre of aqueous solution. Heparin was dissolved in SIF prior to use. Chitosan/siRNA-FAM complexes were added to either the reconstituted mucins to give a final mucin concentration of 0-2% w/v, or to the heparin solution and incubated for 30min at room temperature. Samples were analyzed in a black 96-well plate using a fluorescence spectrometer plate reader (SpectraMax M3, Molecular Devices) set to excitation at 488nm and emission at 520 nm with a longpass cut off filter at 515 nm. Emission spectra were recorded in cuvettes with a path length of 1 cm using the same fluorescence spectrometer (SpectraMax M3).

Gel electrophoresis assays

Chitosan/siRNA-FAM complexes were added to either the reconstituted mucins to give a final mucin concentration of 0-2% w/v, or to the heparin solution and incubated for 30 min at room temperature. Electrophoresis analyses were performed in a 15% native polyacrylamide gel (50 mM Tris, 45 mM Boric Acid, 0.5 mM EDTA) (Mini-Protean, Biorad) at 130 V for 70 min. The gel was stained with 0.5 μg/mL EtBr (Sigma Aldrich) for 20 min and visualized under a UV lamp.

Microfluidic device fabrication and operation

The microfluidic device was fabricated as previously described[27], except that the location of the "push down" valve previously positioned ~450 μm from the mucin and flow channels has been moved to several mm away, enabling a long mucin barrier through which the decomplexed siRNA can diffuse. As previously described[27], a sample of 1.5% (w/v) mucin dissolved in a 20 mM Hepes, 20 mM NaCl, pH 7 buffer containing 0.0007% (w/v) of 500 nm fluorescent microspheres (Polysciences Inc., Warrington, PA) was filled into the device and shaped into a barrier filling the mucin channel. A flow containing the polyplexes was then pumped by gravity into the device (flow direction indicated by arrow in Figure 3a). The polyplexes delivered by this flow then interacted with the mucin barrier. The decomplexation of the polyplexes, release of siRNA, and transport of siRNA into the mucin layer was monitored by fluorescence microscopy.

3. Results and discussion

First, we evaluated the sensitivity of our fluorescence activation system for measuring nanocarrier integrity and stability. Xanthene type dyes, such as fluorescein, are known to self-quench at high densities. Carboxyfluorescein (FAM) is a derivative of fluorescein with shared spectral properties such as small Stokes shift, large extinction coefficient and high quantum

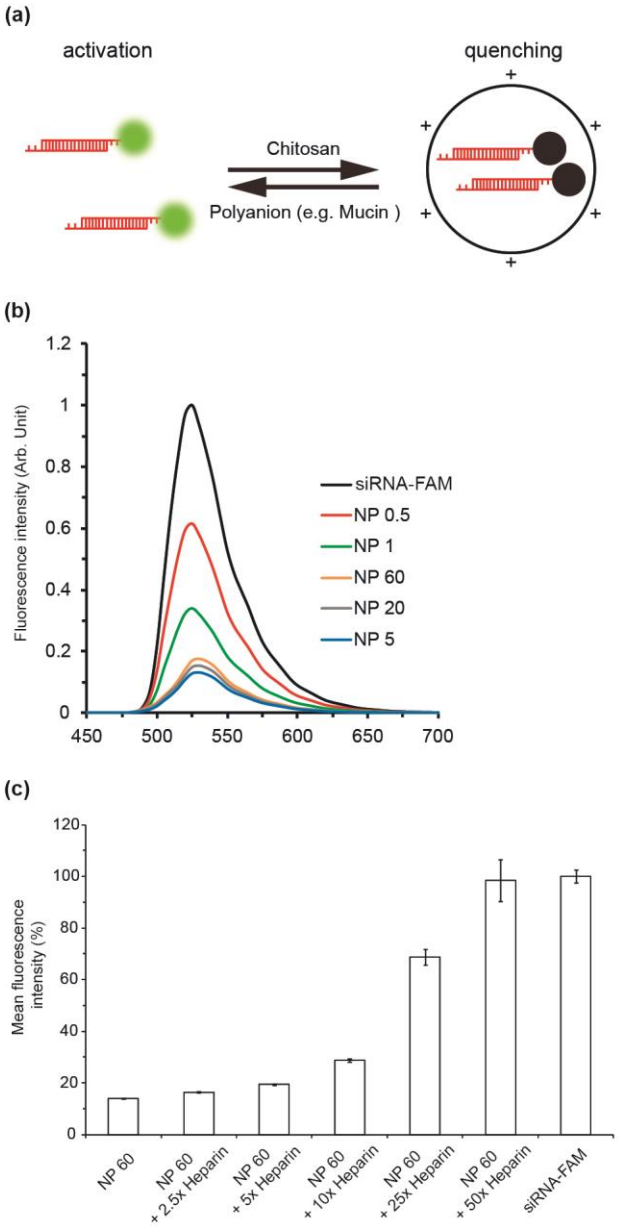

Fig. 1 (a) Schematic representation of the fluorescence activation-based reporter system showing fluorescence quenching upon siRNA complexation with chitosan and fluorescence activation on siRNA release after polyanion challenge. (b) Fluorescence emission spectra measured at 485 nm excitation of chitosan/siRNA-FAM complexes of different amino/phosphate (NP) ratio of 5 (blue), 20 (grey), 60 (orange), 1 (green), 0.5 (red), 0 (black). (c) Normalised fluorescence emission of chitosan/siRNA-FAM complexes of NP 60 after incubation for 30 min with varying amounts of heparin (w/w heparin/siRNA-FAM).

yield.[30] Close proximity of two identical siRNA-FAM molecules mediated by the complexation process with chitosan results in fluorophore interaction and consequent quenching of the fluorescence emission. Conversely, dissociation of the complex and siRNA liberation restores the fluorescent signal, schematically represented in Figure 1a.

We use the fluorescence emission increase at 520 nm as a measure of nanocarrier disassembly. An advantage of our fluorescence activation-based system is the requirement for only one fluorophore instead of the conventional two fluorophore Förster Resonance Energy Transfer (FRET) systems.[17, 31-33] The Förster distance (R_0) for the FAM/FAM pair was calculated to 54 Å using the Förster formalism[25] in accordance with the previously reported value for fluorescein.[30, 34] The hydrodynamic size of the chitosan/siRNA-FAM formulations were determined by photon correlation spectroscopy with diameters ranging from 221.3±6.1 nm to 423.3±15.6 nm that increased at higher NP ratio (Table 1), possibly reflecting the increased chitosan content.

Table 1 Hydrodynamic radius and zeta potential of chitosan/siRNA-FAM polyplexes.

Formulation	Hydrodynamic radius (nm)[a]	Zeta potential (mV)[a]
NP 60	423.3±15.6	21.2±0.9
NP 20	281.3±1.8	19.6±1.5
NP 5	221.3±6.1	21.1±0.6

[a] Size and zeta potential average of three determinations, (±) denote SD.

Zeta potential measurements showed a net positive surface charge above 19 mV. (Table 1) that reflects excess chitosan above an NP ratio of 1. Zeta potential measures charge at the particle surface, however, does not measure the level of polycation. Similar positive zeta potential values were, therefore, observed in nanoparticles with excess chitosan at the particle surface. This is in accordance with previous work from our group[6]. Zeta potential and size was not measured for NP<5 since discrete particles are not formed at NP 1 and NP 0.5. All the investigated formulations showed effective quenching of the fluorescence signal, compared to free siRNA-FAM, as observed from the emission spectra (Figure 1b). Decreasing the NP ratio to 1 compromised the assembly of discrete particles dynamic light scattering (data not shown). A retained fluorescence signal at levels lower than free siRNA-FAM, however, suggests some degree of complexation even at the low NP 1 ratio. This is in accordance with our previous studies on chitosan/siRNA nanoparticles that exhibited open structures and decreased electrophoretic retardation at low NP ratios.[7] Although the emission peaks for NP 5, 20 and 60 are more similar than found between NP 0.5 and 1, differences do exist between NP 5, 20 and 60 that could indicate less tightly bound siRNA at higher NP possibly as a consequence of changes in particle rigidity.

To evaluate the sensitivity of the reporter assay following siRNA displacement, nanocarriers at NP 60 were incubated with varying amounts of heparin (Figure 1c). This addition of polyanionic species such as heparin is an established method to displace nucleic acids from polyplexes as a consequence of polyanionic high charge density.[17, 31] Increased heparin (w/w heparin/siRNA-FAM) resulted in higher fluorescent signals suggesting decomplexation and concomitant siRNA release. A heparin/siRNA w/w ratio of 50 resulted in a fluorescent intensity equal to free siRNA-FAM, suggesting complete decomplexation and siRNA release. The complete decomplexation was confirmed by an electrophoresis assay (see Supplementary Information S1†). The significant difference in fluorescence intensity between intact nanocarriers (NP 5, 20 and 60), non-discrete nanocarriers (NP 0.5 and NP 1) and free siRNA-FAM (Figure 1b), combined with the capability to restore the siRNA-FAM fluorescent signal

by polyanion displacement (Figure 1c) validates our fluorescent activation approach to study the effect of porcine gastric mucin interactions on particle stability over a range of NP ratios.

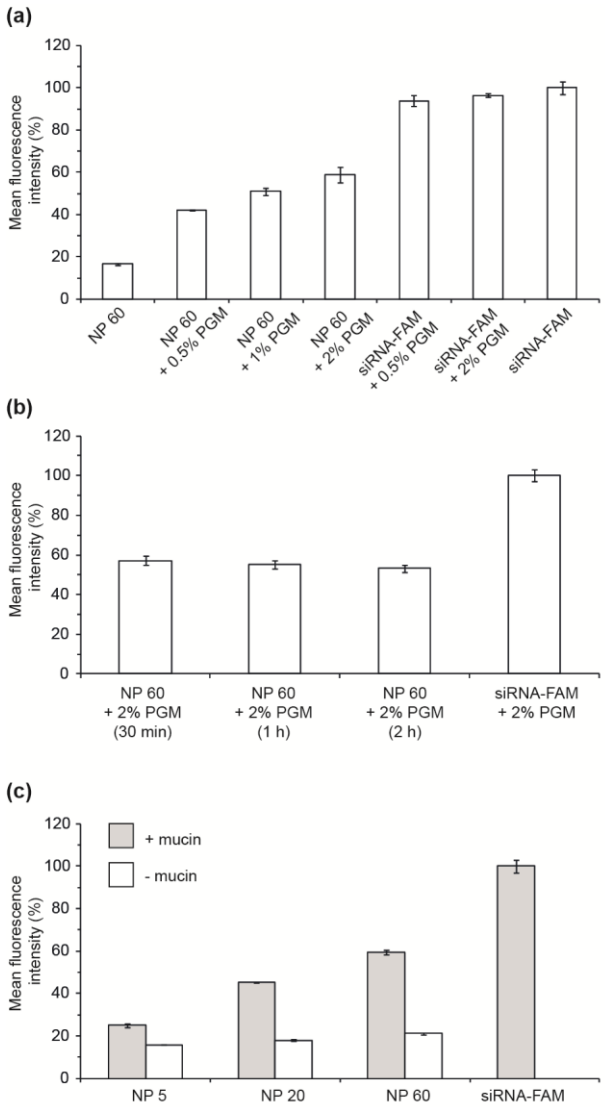

Fig. 2 (a) Normalized fluorescence of chitosan/siRNA-FAM nanocarriers at NP 60 following incubation for 30 min with different amounts (w/v) of porcine gastric mucins (0.5% w/v – 2% w/v) (b) Normalised fluorescence of chitosan/siRNA-FAM complexes at NP 60 after varying incubation times with 2% w/v porcine gastric mucins (c) Normalized fluorescence of chitosan/siRNA-FAM complexes of NP 5, 20 and 60 after incubation for 30 min with 2% w/v porcine gastric mucins (grey bars) or without mucins (white bars). All samples were performed in triplicates. Error bars denote the standard deviation.

Polyplex nanocarriers are disassembled by mucin interactions

Based on the structure and biochemical composition of mucins, possible binding sites for polycationic nanocarriers are neuraminic acid and sulfate groups with pKa values between 2.0 – 2.5[26] which exhibit a negative charge at intestinal physiological conditions of ~pH 7. Electrostatic interaction between the positively charged chitosan and the negatively charged binding sites of the mucin fibers are likely to cause particle dissociation due the competitive forces of the mucin for the chitosan in a similar manner as the heparin polyanionic displacement assay. Our results show a 2.6 to 3.6-fold increase in the normalized fluorescence intensity compared to the fluorescence intensity of nanocarriers alone when nanocarriers of NP 60 were incubated for 30 min with mucin concentrations ranging from 0.5% w/v to 2% w/v (Figure 2a), suggesting mucins are capable of decomplexing the nanocarriers.

The slight increase in fluorescence signal with increasing amount of mucin is possibly due to increase in interaction sites in the mucin gel at higher concentrations. Gel electrophoresis revealed the same trend with the total reconstitution of the siRNA band at a mucin concentration of 2% w/v (see Supplementary Information S2†). Normalized fluorescence for particles at NP 60 in 2% w/v mucin was 3.6-fold higher than NP 60 without mucin, but 1.7-fold lower than free siRNA-FAM in 2% w/v mucins (Figure 2a), that may indicate a mixture of partly disassembled nanocarriers and free siRNA-FAM. It is furthermore important to determine the kinetics of polyplex disassembly in mucins in order to design therapeutic dosing strategies in patients. A constant maximal emission was observed with NP 60 nanocarriers in the prescence of 2% w/v mucins at 30 min, 1 h or 2 h (Figure 2b). Collectively, these results show that maximal disassembly correlates with the highest mucin concentration, and the release remains constant within 30 min. The thickness and integrity of the mucus layer can be compromised under various pathological conditions with an increase in mucus thickness, for example, observed in Asthma,[35] Cystic Fibrosis[36] and Chronic Obstructive Pulmonary Disease,[37] whilst a decrease in thickness observed in Ulcerative Colitis.[38] The observations that greater disassembly is observed at the highest mucin concentration suggests a triggered release mechanism of particle disassembly and consequent siRNA release might be more apparent prior to IBD onset where the mucus barrier remains unaltered.

Nanocarrier formulation influences disassembly

In vitro studies have indicated that high NP ratio (>20) polyplexes are optimal for cellular internalization due to a combination of discrete particle formation[7] and the presence of excess polycation[18] and, have proved, suitable for *in vivo* translation.[8, 39] It is, however, relevant to study the effect of NP ratio on nanocarrier stability in the presence of mucins to predict the performance of nanocarriers at different NP ratios in the GI tract. Changing the NP ratio had a profound effect on the peak emission after 30 min incubation in 2% w/v mucin with increased emission surprisingly exhibited at higher NP ratio (Figure 2c) that could be attributed to a more tightly bound complex at NP 5 and 20 indicated by the lower peak emission than for NP 60 (Figure 1b). Assuming that the siRNA exists in two states *i)* bound in the intact nanocarrier or *ii)* in a non-bound state the maximal release of free siRNA can be estimated according to eq. 1

$$\Phi = (F_{Disassembly} - F_{Bound})/(F_{Free} - F_{Bound}) \quad (1)$$

where Φ is the fraction of free siRNA-FAM, F_{Free} is the maximal fluorescence emission from free siRNA-FAM, F_{Bound} is the maximal fluorescence emission from discrete chitosan/siRNA-FAM nanocarriers and $F_{Disassembly}$ is the maximal fluorescence emission from the disassembled nanocarrier. The calculated maximal siRNA release of 11% (NP 5), 33.2% (NP 20) and

48.6% (NP 60) does not take into account the possibility of partially disassembled nanocarriers, hence the amount of completely free siRNA might be lower than our calculated

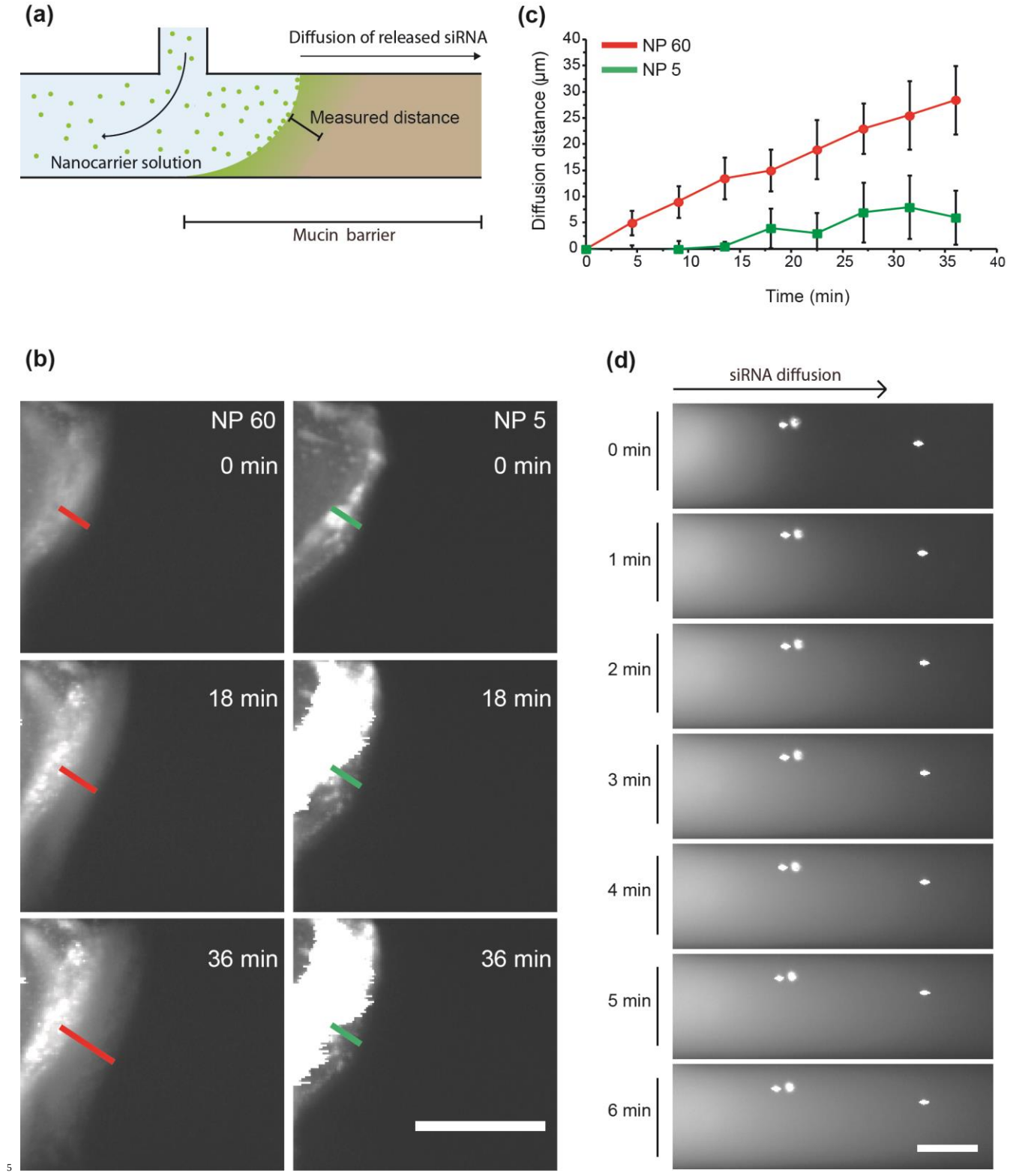

Fig. 3 (a) Schematic representation of the microfluidic mucin barrier *in vitro* model (b) Fluorescent images showing diffusion into the mucin barrier over time indicated by arrows perpendicular to the mucin/liquid interface for chitosan/siRNA-FAM nanocarriers at NP 60

(left, red arrows) and NP 5 (right, green arrows), Scalebar 100 µm. (c) Maximal diffusion distance versus time for chitosan/siRNA-FAM polyplexes of NP 60 (red) and NP 5 (green). Samples were run in triplicates. Error bars denote the standard deviation. (d) Injection of siRNA-FAM in the microfluidic model shows that free siRNA-FAM rapidly penetrates the mucin barrier. Bright fluorescent spot are tracer particles for mucin barrier localization, Scalebar 100 µm.

values. Our results show that the higher NP ratio (NP 60) nanocarriers release more free siRNA after mucin interaction than nanocarriers at lower NP ratio (NP 5 and 20). This suggests that the higher NP ratio nanocarriers are more unstable than low NP ratio nanocarriers even though the opposite trend has previously been shown.[7] These differences could be attributed to the mucin-specific interactions investigated in this work and show the importance of studying site-specific conditions for predicting the biological performance of nanocarriers.

Disassembly results in transport of siRNA into a mucin barrier

The decomplexing of nanocarriers in the presence of mucins may therefore have important implications for *in vivo* siRNA delivery, as the siRNA inside the nanocarriers must traverse the mucus barrier of the body before reaching systemic circulation. We use a modified version of an established microfluidic *in vitro* model of the GI mucus barrier[26, 27], for the first time, to study the dynamic interaction and transit of siRNA nanocarriers at the mucus interface, schematically represented in Figure 3a. Native purified mucins from the pig stomach used previously for predicting mucin gelation properties,[28] mucus barrier function,[26] and particle diffusion in mucin gels[15] was selected for our studies. In the microfluidic device, nanocarriers are delivered by fluid flow to the surface of a mucin layer on-chip, experimentally simulating the process of nanocarrier delivery to the surface of an *in vivo* mucus layer. The transport of the fluorescent siRNA into the mucin barrier is visualized using fluorescence microscopy. Using this device, we measure and compare the dynamic interaction of chitosan/siRNA-FAM NP 5 and chitosan/siRNA-FAM NP 60 nanocarriers with a mucin barrier.

Our results show a distinct accumulation of particles at the mucin/liquid interface after < 5 min following chitosan/siRNA-FAM NP 5 and chitosan/siRNA-FAM NP 60 nanocarrier injection (Figure 3b), suggesting aggregation at the barrier interface resulting from strong interaction between the nanocarrier and the mucins. No aggregation at the mucin/liquid interface was evident after injection of free siRNA-FAM, but surprisingly rapid diffusion into the mucin barrier occurred (Figure 3d), suggesting minimal interactions between free siRNA-FAM and mucins. No transport of siRNA into the mucin barrier was observed over a time period of ~30 min when chitosan/siRNA-FAM NP 5 was injected, but diffusion of siRNA was visualized after chitosan/siRNA-FAM NP 60 into the barrier (Figure 3b). To quantify the release of siRNA from chitosan/siRNA-FAM NP 60, we measure the distance from the mucin/liquid interface to the front of the diffusive entity over time (Figure 3c). A clear difference in diffusion distance versus time is observed between NP 5 and 60 (Figure 3c). The transport rate of the diffused entity from NP 60 nanocarriers was lower than free siRNA, suggesting that the released siRNA may be comprised of partially dissembled particles. Furthermore, although siRNA release was not detected in the case of chitosan/siRNA-FAM NP 5 as measured by microfluidics, siRNA release from chitosan/siRNA-FAM NP 5 nanocarriers did occur in the fluorescence quenching experiment. This small discrepancy may be due to the higher stability of the NP 5 nanocarrier (refer to Figure 2c), resulting in released siRNA below the detection limit of the microfluidics experiment.

Previous to this work, the consensus of opinion is that nanocarrier polyplexes transverse the mucus barrier intact, but direct experimental evidence is lacking. This consensus that polyplexes traverse the mucus barrier intact is further in doubt given recent evidence that most mucoadhesive nanoparticles aggregate to the surface of the mucus barrier without significant penetration.[40] The suggested release and transport of siRNA in the mucus barrier in this work promotes an alternative model of disassembly and consequent transit of intact siRNA. Disassembly and consequent transit of siRNA is further supported by our previous *in vivo* work reporting the detection of a band of siRNA at the luminal site of the intestinal wall and detection of siRNA at systemic sites after oral administration of chitosan/siRNA nanocarriers to mice[12]. Taken together, our findings supporting polyplex disassembly at the mucus interface imply that protection and localization of siRNA in the GI lumen may be conferred by nanoparticles, while it is envisaged that chemical modification such as conjugation to Toll-like receptor agonists[41] or aptamers[42] need to be built into the design of the nucleic acid cargo in order to facilitate cellular entry after release triggered by mucus interaction.

4. Conclusion

We show NP dependent nanocarrier disassembly and subsequent release and transit of siRNA upon interaction with GI mucins that promotes a new model for nanocarrier transport across mucus barriers. The capability for free siRNA to transit across mucin barriers opens up a new type of therapeutic approach based on triggered release of the therapeutic cargo using the mucus barrier itself. Chemical modifications that mediate cellular entry would seemingly need to be built into the design of the siRNA cargo to utilise this approach. This work explains the effect of interaction at the nanoparticle/mucin interface and has important implications for the design and development of self-assembled nucleic acid-based nanocarriers for mucosal disease treatment.

Acknowledgements

This work was carried out at the Department of Biological Engineering, Massachusetts Institute of Technology. We thank Eugene Bell Career Development Professor Katharina Ribbeck for providing facilities together with valuable discussions and insightful suggestions on mucins, Professor Jongyoon Han for providing facilities for conducting the microfluidic experiments and Borja Ballarín-González for the assistance in supplying materials. T.B.T. acknowledges support from the Niels Bohr Foundation. This work was partially supported by the Novo

Nordisk Foundation.

Notes and references

[a]*Interdisciplinary Nanoscience Center (iNANO), Gustav Wieds Vej 14, DK-8000, Aarhus, Denmark. E-mail: troels@inano.au.dk; kenh@inano.au.dk*
[b]*Department of Molecular Biology and Genetics, Aarhus University, Nordre Ringgade 1, DK-8000, Aarhus, Denmark*
[c]*Department of Electrical Engineering and Computer Science, MIT, 77 Massachusetts Avenue, Cambridge, MA, 02139, USA. E-mail: leondn.li@gmail.com*
[d]*Harvard-MIT Division of Health Sciences and Technology, 77 Massachusetts Avenue, Cambridge, MA, 02139, USA*
[e]*Department of Biological Engineering, MIT, 77 Massachusetts Avenue, Cambridge, MA, 02139, USA*

† Electronic Supplementary Information (ESI) available: Additional figures S1 and S2. See DOI: 10.1039/b000000x/

1. S. M. Elbashir, J. Harborth, W. Lendeckel, A. Yalcin, K. Weber and T. Tuschl, *Nature*, 2001, **411**, 494-498.
2. B. L. Davidson and P. B. McCray, *Nat. Rev. Genet.*, 2011, **12**, 329-340.
3. K. A. Howard and J. Kjems, *Expert Opin. Biol. Ther.*, 2007, **7**, 1811-1822.
4. K. A. Howard, *Adv. Drug Del. Rev.*, 2009, **61**, 710-720.
5. C. Abraham and J. H. Cho, *New Engl. J. Med.*, 2009, **361**, 2066-2078.
6. K. Howard, U. Rahbek, X. Liu, C. Damgaard, S. Glud, M. Andersen, M. Hovgaard, A. Schmitz, J. Nyengaard and F. Besenbacher, *Mol. Ther.*, 2006, **14**, 476-484.
7. X. Liu, K. A. Howard, M. Dong, M. Ø. Andersen, U. L. Rahbek, M. G. Johnsen, O. C. Hansen, F. Besenbacher and J. Kjems, *Biomaterials*, 2007, **28**, 1280-1288.
8. K. A. Howard, S. R. Paludan, M. A. Behlke, F. Besenbacher, B. Deleuran and J. Kjems, *Mol. Ther.*, 2008, **17**, 162-168.
9. P. Artursson, T. Lindmark, S. S. Davis and L. Illum, *Pharm. Res.*, 1994, **11**, 1358-1361.
10. L. Illum, *Pharm. Res.*, 1998, **15**, 1326-1331.
11. R. J. Soane, M. Frier, A. C. Perkins, N. S. Jones, S. S. Davis and L. Illum, *Int. J. Pharm.*, 1999, **178**, 55-65.
12. B. Ballarín-González, F. Dagnaes-Hansen, R. A. Fenton, S. Gao, S. Hein, M. Dong, J. Kjems and K. A. Howard, *Mol. Ther. — Nucleic Acids*, 2013, **2**, e76.
13. M. E. V. Johansson, H. Sjövall and G. C. Hansson, *Nat. Rev. Gastroenterol. Hepatol.*, 2013, **10**, 352-361.
14. R. A. Cone, *Adv. Drug Del. Rev.*, 2009, **61**, 75-85.
15. O. Lieleg, I. Vladescu and K. Ribbeck, *Biophys. J.*, 2010, **98**, 1782-1789.
16. A. I. Sogias, A. C. Williams and V. V. Khutoryanskiy, *Biomacromolecules*, 2008, **9**, 1837-1842.
17. M. Thibault, S. Nimesh, M. Lavertu and M. D. Buschmann, *Mol. Ther.*, 2010, **18**, 1787-1795.
18. M. Thibault, M. Astolfi, N. Tran-Khanh, M. Lavertu, V. Darras, A. Merzouki and M. D. Buschmann, *Biomaterials*, 2011, **32**, 4639-4646.
19. J. N. Weinstein, Y. Yoshikami, P. Henkart, R. Blumenthal and W. A. Hagins, *Science*, 1977, **195**, 489-492.
20. A. Stutzin, *FEBS Lett.*, 1986, **197**, 274-280.
21. L. J. Jones, R. H. Upson, R. P. Haugland, N. Panchuk-Voloshina, M. Zhou and R. P. Haugland, *Anal. Biochem.*, 1997, **251**, 144-152.
22. X. Zhuang, T. Ha, H. D. Kim, T. Centner, S. Labeit and S. Chu, *Proc. Natl. Acad. Sci. USA*, 2000, **97**, 14241-14244.
23. K. Zhou, H. Liu, S. Zhang, X. Huang, Y. Wang, G. Huang, B. D. Sumer and J. Gao, *J. Am. Chem. Soc.*, 2012, **134**, 7803-7811.
24. L.-C. Ho, C.-M. Ou, C.-L. Li, S.-Y. Chen, H.-W. Li and H.-T. Chang, *J. Mater. Chem. B*, 2013, **1**, 2425-2432.
25. J. R. Lakowicz, *Principles of Fluorescence Spectroscopy*, Springer, 2006.
26. L. Li, O. Lieleg, S. Jang, K. Ribbeck and J. Han, *Lab Chip*, 2012, **12**, 4071.
27. L. D. Li, T. Crouzier, A. Sarkar, L. Dunphy, J. Han and K. Ribbeck, *Biophys. J.*, 2013, **105**, 1357-1365.
28. J. P. Celli, B. S. Turner, N. H. Afdhal, R. H. Ewoldt, G. H. McKinley, R. Bansil and S. Erramilli, *Biomacromolecules*, 2007, **8**, 1580-1586.
29. M. Ø. Andersen, K. A. Howard and J. Kjems, *Methods Mol. Cell. Biol.*, 2009, **555**, 77-86.
30. L. W. Runnels and S. F. Scarlata, *Biophys. J.*, 1995, **69**, 1569-1583.
31. N. P. Gabrielson and D. W. Pack, *Biomacromolecules*, 2006, **7**, 2427-2435.
32. Y.-P. Ho, H. H. Chen, K. W. Leong and T.-H. Wang, *J. Control. Release*, 2006, **116**, 83-89.
33. C. A. Alabi, K. T. Love, G. Sahay, T. Stutzman, W. T. Young, R. Langer and D. G. Anderson, *ACS Nano*, 2012, **6**, 6133-6141.
34. J. R. Lakowicz, J. Malicka, S. D'Auria and I. Gryczynski, *Anal. Biochem.*, 2003, **320**, 13-20.
35. L. Cohn, *J. Clin. Invest.*, 2006, **116**, 306-308.
36. A. S. Verkman, Y. Song and J. R. Thiagarajah, *Am. J. Physiol. Cell Physiol.*, 2003, **284**, C2-C15.
37. J. C. Hogg, F. Chu, S. Utokaparch, R. Woods, W. M. Elliott, L. Buzatu, R. M. Cherniack, R. M. Rogers, F. C. Sciurba, H. O. Coxson and P. D. Pare, *New Engl. J. Med.*, 2004, **350**, 2645-2653.
38. R. D. Pullan, G. A. O. Thomas, M. Rhodes, R. G. Newcombe, G. T. Williams, A. Allen and J. Rhodes, *Gut*, 1994, **35**, 353-359.
39. E. J. B. Nielsen, J. M. Nielsen, D. Becker, A. Karlas, H. Prakash, S. Z. Glud, J. Merrison, F. Besenbacher, T. F. Meyer, J. Kjems and K. A. Howard, *Pharm. Res.*, 2010, **27**, 2520-2527.
40. L. M. Ensign, B. C. Tang, Y. Y. Wang, T. A. Tse, T. Hoen, R. Cone and J. Hanes, *Sci. Transl. Med.*, 2012, **4**, 138ra179.
41. M. Kortylewski, P. Swiderski, A. Herrmann, L. Wang, C. Kowolik, M. Kujawski, H. Lee, A. Scuto, Y. Liu, C. Yang, J. Deng, H. S. Soifer, A. Raubitschek, S. Forman, J. J. Rossi, D. M. Pardoll, R. Jove and H. Yu, *Nat. Biotechnol.*, 2009, **27**, 925-932.
42. L. A. Wheeler, R. Trifonova, V. Vrbanac, E. Basar, S. McKernan, Z. Xu, E. Seung, M. Deruaz, T. Dudek, J. I. Einarsson, L. Yang, T. M. Allen, A. D. Luster, A. M. Tager, D. M. Dykxhoorn and J. Lieberman, *J. Clin. Invest.*, 2011, **121**, 2401-2412.